The International Journal of Advanced Manufacturing Technology (2019) 104:3773–3786
https://doi.org/10.1007/s00170-019-04049-7

ORIGINAL ARTICLE

Structural dynamic design optimization and experimental verification of a machine tool

Lei Shen[1] · Xiaohong Ding[1] · Tianjian Li[1] · Xiangzhi Kong[2] · Xiaohu Dong[1]

Received: 9 March 2019 / Accepted: 18 June 2019 / Published online: 19 July 2019

Abstract

Structural dynamic performance of a machine tool greatly affects machining precision and productivity. One effective approach in improving the dynamic performance is by applying topology design optimization to the machine tool structure. However, traditional topology optimization method is hard to implement and does not provide a clear stiffener layout. Furthermore, the topology optimization of certain components does not signify the performance improvement of a holistic machine tool. This paper suggests a new structural dynamic design optimization method for the holistic machine tool. The Adaptive Growth Method which is based on the growth mechanism of natural branch systems is adopted to design the inner stiffener layout of structures, and an optimization strategy for the holistic machine tool utilizing dynamic sensitivity analysis is studied. Both components and contact parts are considered. The dynamic sensitivities of the components are analyzed based on modal test data, and help to determine which components need to be optimized. Then, the headstock, column, and bed are optimized, and the weak contact stiffness is improved. The FEA (finite element analysis) results of an optimized machine tool show that the TCP (tool center point) harmonic displacement is decreased distinctly. To validate the effectiveness of the suggested method, an experiment of the manufactured machine tool structure is conducted, and the experimental results had shown great improvements in the holistic machine tool.

Keywords Machine tool structure · Dynamic performance · Topology optimization · Dynamic sensitivity analysis · Modal test

1 Introduction

The structural dynamic performance of the machine tool is a key factor that affects the machining precision and productivity. Structural design optimization is a type of crucial approach to improve the dynamic performance of the machine tool structures and maximize the utilization ratio of materials [1–4]. Because some key components of the machine tool are box structures such as bed, column, and headstock, the layout of inside stiffeners in these structures plays an indispensable role to improve the structural performance. The most effective design method to obtain the optimal layout of inside stiffeners in box structures is the structural topology optimization, which concerns to the optimal distribution of materials for load-bearing structures [5]. Among the developed topology optimization methods, SIMP [6] (Solid Isotropic Material with Penalization) scheme is widely used in the machine tool structure. Drude et al. [7] applied topology optimization to derive an optimum ribbing structure of large forming tools. Yun et al. [8] optimized large structural components based on a response surface model. Chen et al. [9] employed topology and size optimization techniques to improve the design of a machining center rib, considering static and dynamic constraints. Law et al. [10] modified the column by topology optimization and improved the dynamic performance of the machine tool. However, these design results given by the SIMP method are primarily patterns of material density distribution, which are difficult to identify the real stiffener layout, and the topological forms usually are too complex to manufacture [11]. To overcome these limitations, Ding and Yamazaki [12, 13] proposed a bionic topology optimization method based on the growth mechanism of biological branch systems in nature, which is called Adaptive Growth Method. This method can obtain a clear layout of

✉ Xiaohong Ding
dingxh@usst.edu.cn

[1] School of Mechanical Engineering, University of Shanghai for Science and Technology, Shanghai 200093, China

[2] Shenyang Machine Tool (Group) Design and Research Institute, Shenyang 110142, China

stiffeners and is friendly to manufacture. Adaptive Growth Method has been applied to the layout design of stiffeners in plate/shell structures [14] and machine pedestal structures [15–17].

However, the topology optimization of certain components or parts does not signify the performance improvement of the holistic machine tool. If a machine tool is broken down into its structural parts and each part is optimized individually or blindly, it may be limited in improving the performance of the holistic machine tool [18, 19]. It is ideal to optimally design the holistic machine tool, but topology design optimization of the holistic machine tool structure is hard to implement in general due to the large numbers of design variables and difficult definition of contact parts between components. One effective approach is the topology design optimization of single component which is identified as the weak part of the holistic machine tool [20]. However, the weak component is often identified by experiment estimation or simple analysis, which lacks of efficient theoretical explanation. Such solution can improve the dynamic performance of the machine tool to a certain extent, but has limitation. For further improvement, the design optimization strategy of the machine tool should be reconsidered. He et al. [21] employed modal mass distribution matrix to identify the weak components of the machine tool, but did not offer a solution for structural optimization.

Dynamic sensitivities of the components reveal the influence of structural parameters of the components on the dynamic performance of the machine tool, and it is possible to determine which components need to be optimized and offer effective guide to the design optimization strategy of the holistic machine tool. Liang and Chen [22, 23] studied the influence of mechanical components on the machining performance of a fly-cutting machine tool. Li et al. [24] analyzed the influence of mass and stiffness of spindle with respect to dynamic error in a cutting tool system and figured out the optimal mass and stiffness of spindle. Zhao et al. [25] introduced a new dynamic sensitivity approach based on error propagation model, and increased the stiffness of sensitive error component and improved the static stiffness of the machine tool. However, this dynamic sensitivity analysis mainly concentrates on a certain part or component, which is short for the overall consideration of the holistic machine tool structure; thus, the dynamic performance improvement has limitation. Furthermore, these sensitivities are usually analyzed with FEA or theoretical model in most cases. Because the accurate FEA model is difficult to establish and the theoretical models are based on some hypothesis, the dynamic sensitivity analysis has limited accuracy.

On the other hand, about 60% of the dynamic stiffness in a holistic machine tool structure originates in the contact parts [26]. Deng et al. [27] developed a joint stiffness configuration to optimize the dynamic characteristics of the machine tool. Hung et al. [28, 29] analyzed the effect of preload linear guide and spindle bearings on the dynamic performance of a horizontal machining center. Hence, it is possible to improve the dynamic performance of the machine tool by increasing the stiffness of contact parts, and the dynamic performance can be further improved if both component structures and contact parts are considered simultaneously.

This paper suggests a new structural dynamic design optimization method of the holistic machine tool. Adaptive Growth Method is adopted to design the inside stiffeners of machine tool components, and a design optimization strategy for the holistic machine tool is studied utilizing the dynamic sensitivity analysis, and both components and contact parts are considered. The dynamic sensitivity analysis of the components is first done, which is based on modal test data on account of the limited accuracy of FEA model. The sensitivity analysis results are used to determine which components need to be optimized and the component rankings for stiffness improvement and mass reduction. At the same time, the weak contact parts are also identified through stiffness sensitivity analysis. Thus, the design optimization strategy of the machine tool is worked out. In terms of the optimization strategy, the structural topology optimization of the components is conducted by utilizing Adaptive Growth Method. The stiffness of the components is increased, and the mass is reduced. The weak contact stiffness is improved by increasing the contact area meanwhile. Finally, the optimal machine tool structure is obtained, and the dynamic performance is improved dramatically through FEA simulation. To further verify the performance, the optimized machine tool structure is manufactured, and the experiments provide strong supportive results.

This work is organized as follows. In Section 2, sensitivity analysis is conducted which includes the dynamic sensitivity analysis of the components and stiffness analysis of contact parts. Component rankings for mass reduction and stiffness improvement are determined, and the weak contact stiffness is identified as well. Then, the dynamic design optimization strategy of the holistic machine tool is summarized. Section 3 describes the topology optimization process of the components utilizing Adaptive Growth Method and also gives a brief introduction of the design method. The FEA and experiment verifications for the holistic machine tool are provided in Section 4. Finally, conclusions are given in Section 5.

2 Sensitivity analysis

2.1 Dynamic sensitivity analysis of the components

Regarding eigenfrequency as the indicator of the dynamic performance of the machine tool, the dynamic sensitivity is defined as the change rate of eigenfrequency of the machine tool with respect to structural parameters, which include the mass, stiffness, or damping of the components.

The free vibration characteristic equation is

$$\left(\mathbf{K}-\omega_r^2\mathbf{M}\right)\boldsymbol{\Psi}_r = 0 \tag{1}$$

where $\mathbf{K}$ and $\mathbf{M}$ are stiffness and mass matrix, respectively. $\boldsymbol{\Psi}_r$ and ω_r are modal vector and eigenfrequency of r-th mode, respectively. The derivative of Eq. 1 with respect to the structural design parameter p is

$$\frac{\partial \mathbf{K}}{\partial p}\boldsymbol{\Psi}_r - 2\omega_r \mathbf{M}\boldsymbol{\Psi}_r \frac{\partial \omega_r}{\partial p} - \omega_r^2 \frac{\partial \mathbf{M}}{\partial p}\boldsymbol{\Psi}_r = 0 \tag{2}$$

Then

$$\frac{\partial \omega_r}{\partial p} = \frac{1}{2\omega_r}\left(\boldsymbol{\Psi}_r^{\mathrm{T}}\frac{\partial \mathbf{K}}{\partial p}\boldsymbol{\Psi}_r - \omega_r^2\boldsymbol{\Psi}_r^{\mathrm{T}}\frac{\partial \mathbf{M}}{\partial p}\boldsymbol{\Psi}_r\right) \tag{3}$$

Using stiffness element k_{ij} of $\mathbf{K}$ to substitute p, where i and j represent the matrix coordinate. Then

$$\frac{\partial \omega_r}{\partial k_{ij}} = \frac{1}{2\omega_r}\boldsymbol{\Psi}_r^T\frac{\partial \mathbf{K}}{\partial k_{ij}}\boldsymbol{\Psi}_r \tag{4}$$

$$\frac{\partial k_{ij}}{\partial k_{ji}} = \frac{\partial k_{ji}}{\partial k_{ij}} = 1 \tag{5}$$

When $i \neq j$

$$\phi_r^T\frac{\partial \mathbf{K}}{\partial k_{ij}}\phi_r = [\phi_1\,\phi_2 \ldots \phi_N]_r \begin{bmatrix} 0 & \cdots & I_{ij} & \cdots \\ \vdots & 0 & & \\ I_{ji} & & \ddots & \\ & & & 0 \end{bmatrix} \begin{bmatrix} \phi_1 \\ \phi_2 \\ \vdots \\ \phi_N \end{bmatrix}_r = 2\phi_{ir}\phi_{jr} \tag{6}$$

When $i = j$

$$\phi_r^T\frac{\partial \mathbf{K}}{\partial k_{ij}}\phi_r = [\phi_1\,\phi_2 \ldots \phi_N]_r \begin{bmatrix} 0 & & & 0 \\ & I_{ij} & & \\ & & \ddots & \\ 0 & & & 0 \end{bmatrix} \begin{bmatrix} \phi_1 \\ \phi_2 \\ \vdots \\ \phi_N \end{bmatrix}_r = \phi_{ir}^2 \tag{7}$$

Combining these two situations, sensitivity of eigenfrequency with respect to stiffness element k_{ij} is

$$\frac{\partial \omega_r}{\partial k_{ij}} = \begin{cases} \Psi_{ir}\Psi_{jr}/\omega_r & (i \neq j) \\ \Psi_{ir}^2/2\omega_r & (i = j) \end{cases} \tag{8}$$

As the same way of Eq. 8, sensitivity of eigenfrequency with respect to mass element m_{ij} of $\mathbf{M}$ is derived as

$$\frac{\partial \omega_r}{\partial m_{ij}} = \begin{cases} -\omega_r\Psi_{ir}\Psi_{jr} & (i \neq j) \\ -\frac{1}{2}\omega_r\Psi_{ir}^2 & (i = j) \end{cases} \tag{9}$$

The sensitivities of eigenfrequency of the machine tool with respect to stiffness and mass of each element can be calculated utilizing Eqs. 8 and 9. In the process of modal test, all acceleration sensors are installed on the primary components of the machine tool. Each acceleration sensor mounted on the surface of component is treated as a test element of the machine tool, and the modal test data of all test elements can be obtained by the modal test. If n acceleration sensors are mounted on certain component of the machine tool, such as bed and column, the sensitivities with respect to the stiffness and mass of this component can be assembled by the sensitivities of all test elements on this component by adopting statistical principles, which are expressed as

$$\begin{aligned} \alpha_{\mathrm{k}} &= \sqrt{\left(\alpha_{\mathrm{k1}}^2 + \alpha_{\mathrm{k2}}^2 + \cdots + \alpha_{\mathrm{kn}}^2\right)/n} \\ \alpha_{\mathrm{m}} &= -\sqrt{\left(\alpha_{\mathrm{m1}}^2 + \alpha_{\mathrm{m2}}^2 + \cdots + \alpha_{\mathrm{mn}}^2\right)/n} \end{aligned} \tag{10}$$

where α_k and α_m represent the sensitivities with respect to the stiffness and mass of the component, respectively, and α_{kn} and α_{mn} indicate the sensitivities with respect to stiffness and mass of n-th test element of the component, respectively. Positive sensitivity with respect to stiffness means a positive correlation between eigenfrequency and stiffness, while the negative sensitivity with respect to mass indicates a negative correlation between eigenfrequency and mass. Employing Eq. 10, the sensitivities with respect to stiffness and mass of each component are calculated. Through the dynamic sensitivity analysis, it is convenient to determine which components need to be optimized, and the component rankings for stiffness improvement and mass reduction. Consequently, the optimal distributions of stiffness and mass of the components are figured out.

Consider a vertical machining center shown in Fig. 1. The structural components are headstock, spindle, column, bed, saddle, and table. The modal test is shown in Fig. 2. In the test, 98 three-axis acceleration sensors are mounted to measure the vibration response under a random vibration environment. Typical test elements of the machine tool are shown in Fig. 3, and all 13 test elements of headstock are shown completely. Then, the eigenmodes and eigenfrequencies of the machine tool are identified by

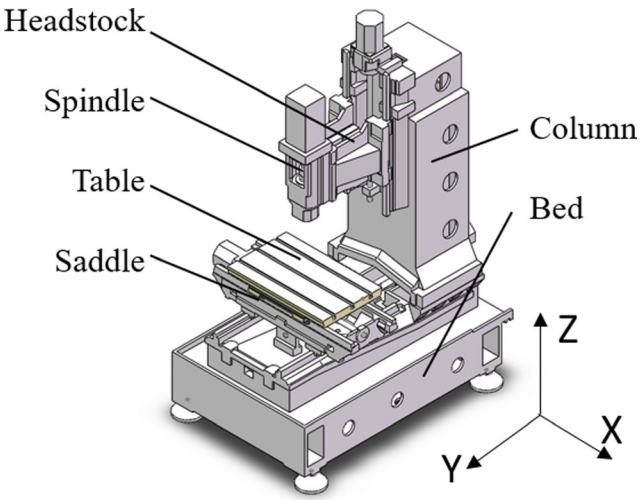

Fig. 1 Sketch map of the machine tool structure

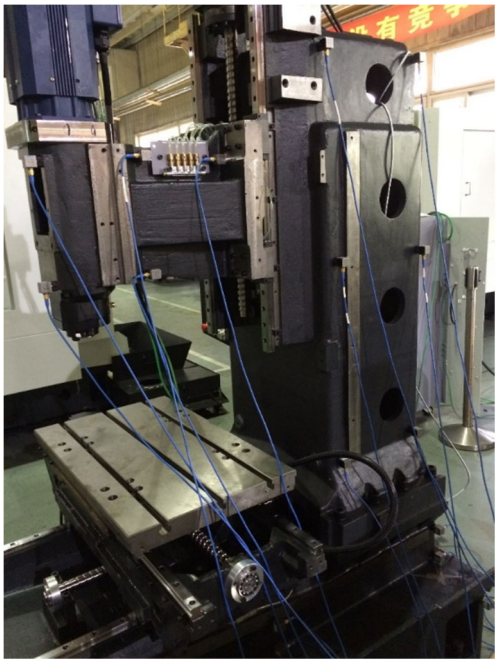

Fig. 2 Modal test onsite of the machine tool

analyzing the frequency response functions (FRFs). The eigenfrequencies of the lowest 6 modes are shown in Table 1. First mode amplitude of test elements of headstock is expressed in Eq. 11, where the row means the number of test element of headstock, and the column represents the coordinate axis.

Table 1 Eigenfrequencies of the lowest 6 modes from modal test

Mode	Eigenfrequency/Hz
1	37.4
2	89.3
3	98.3
4	134.0
5	160.8
6	175.5

Utilizing Eq. 9, the sensitivity of first eigenfrequency of the machine tool with respect to mass of each element is calculated. The typical sensitivities are shown in Fig. 4 with histogram, and the number of X coordinate represents the test element number of certain component, which is kept constant with that in Fig. 3. Adopting Eq. 10, the sensitivity with respect to mass of each component is calculated, which is the red lines in Fig. 4. The sensitivity magnitudes with respect to mass of headstock, column, bed, saddle, and table are 4.47×10^{-6}, 3.58×10^{-6}, 7.88×10^{-7}, 7.52×10^{-7}, and 1.67×10^{-7} rad/(s kg), respectively. Therefore, the component ranking for mass reduction is headstock, column, bed, saddle, and table. Similarly, the sensitivity with respect to stiffness of each test element is worked out as shown in Fig. 5, and the sensitivity magnitudes with respect to stiffness of headstock, column, bed, saddle, and table are 2.54×10^{-9}, 2.03×10^{-9}, $4.47 \times$

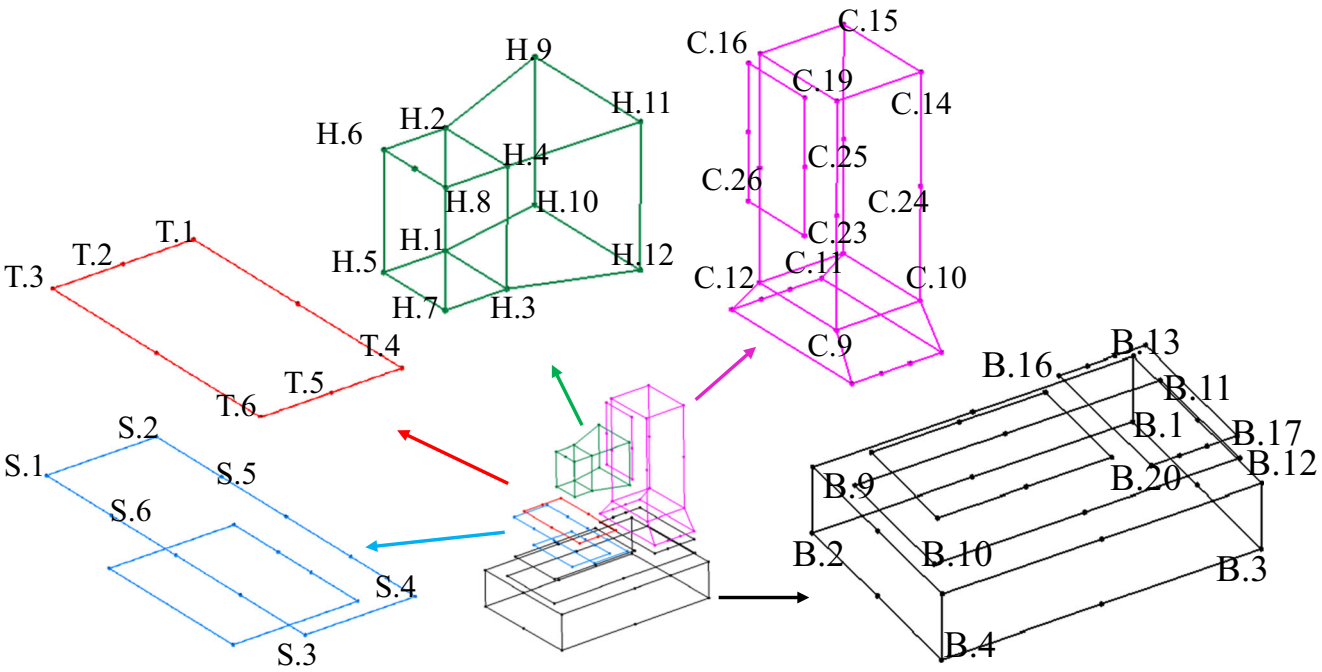

Fig. 3 Typical test elements of the machine tool

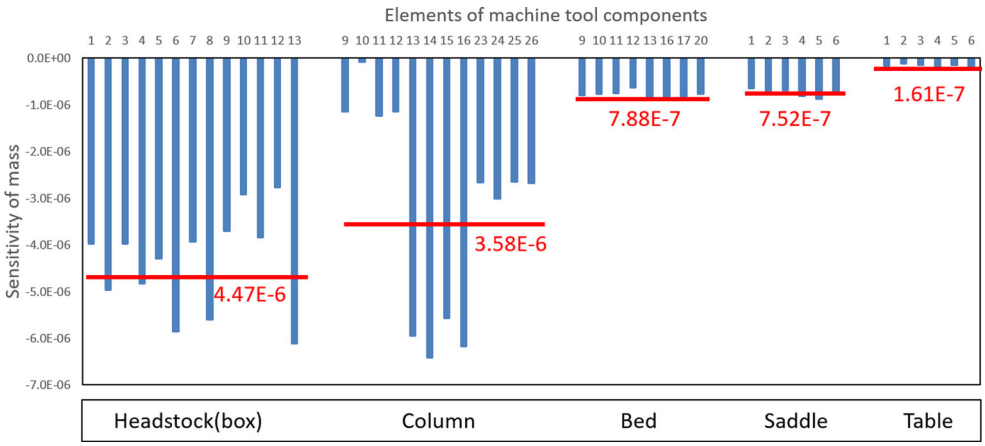

Fig. 4 Sensitivity of first eigenfrequency with respect to mass

10^{-10}, 4.27×10^{-10}, and 9.14×10^{-11} rad m/(s N), respectively, which are the red lines in Fig. 5 as well. It is clear that the component ranking for stiffness improvement is headstock, column, bed, saddle, and table. In addition, the sensitivity magnitudes for saddle and table are much less than those for other components, which implies changing the stiffness or mass of saddle and table has restricted the effect on the dynamic performance of the machine tool; thus, saddle and table are not considered to optimize in this paper.

$$\phi_1 = \begin{pmatrix} 3.7\times10^{-4} & 2.2\times10^{-4} & 6.0\times10^{-5} \\ 4.2\times10^{-4} & 2.3\times10^{-4} & 8.0\times10^{-5} \\ 3.7\times10^{-4} & 2.2\times10^{-4} & 6.0\times10^{-5} \\ 4.2\times10^{-4} & 2.2\times10^{-4} & 7.0\times10^{-5} \\ 3.5\times10^{-4} & 2.8\times10^{-4} & 6.0\times10^{-5} \\ 4.4\times10^{-4} & 2.8\times10^{-4} & 8.0\times10^{-5} \\ 3.4\times10^{-4} & 2.6\times10^{-4} & 6.0\times10^{-5} \\ 4.4\times10^{-4} & 2.6\times10^{-4} & 7.0\times10^{-5} \\ 4.0\times10^{-4} & 9.0\times10^{-5} & 9.0\times10^{-5} \\ 3.4\times10^{-4} & 1.4\times10^{-4} & 6.0\times10^{-5} \\ 4.1\times10^{-4} & 9.0\times10^{-5} & 8.0\times10^{-5} \\ 3.4\times10^{-4} & 1.1\times10^{-4} & 6.0\times10^{-5} \\ 4.6\times10^{-4} & 2.7\times10^{-4} & 8.0\times10^{-5} \end{pmatrix} \quad (11)$$

Synthesizing the above calculation and analysis, the optimization scheme for the components is figured out. The component rankings for the stiffness improvement and mass reduction are as follows: headstock, column, and bed. The extent for the mass reduction and stiffness improvement of headstock is largest, which means the optimization of headstock should be carried out with priority. The following are column and bed.

2.2 Stiffness sensitivity analysis of contact parts

The FEA model of the machine tool is built to study the stiffness of contact parts and evaluate the dynamic performance of the machine tool. On the basis of the structure characteristics of the machine tool, the primary eight contact parts are shown in Fig. 6. K_1 to K_8 represent the contact stiffness, and X, Y, and Z represent the axis directions. Comparison of mode shapes between experimental and FEA models is shown in Fig. 7, and Table 2 exhibits the eigenfrequency comparison. It is apparent that the modal shapes of FEA and the experiment of the machine tool are kept consistent in general, and the eigenfrequency errors of the FEA model are 5.0%, 0.1%, 1.4%, and 1.5% of the

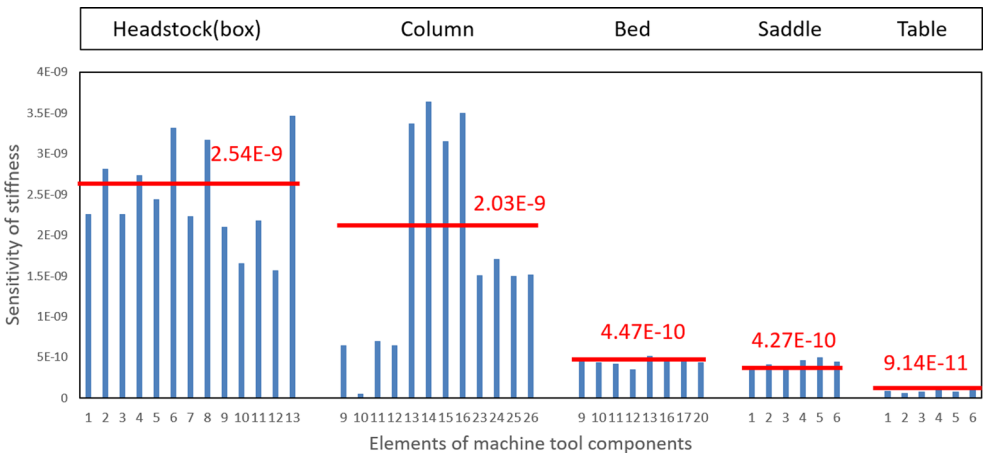

Fig. 5 Sensitivity of first eigenfrequency with respect to stiffness

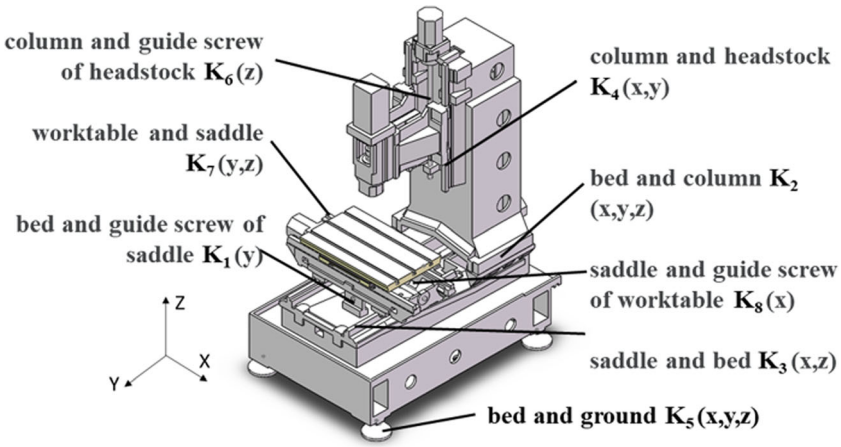

Fig. 6 Contact part definition of the machine tool

lowest 4 modes, respectively. The results indicate that the FEA model of the machine tool is believable.

In order to study the impact of contact parts on the dynamic performance of the machine tool and identify the weak contact stiffness, the sensitivity of the first eigenfrequency of the machine tool with respect to contact stiffness is analyzed as shown in Fig. 8. It is obvious that K_2 (contact stiffness of column and bed), K_4 (contact stiffness of column and headstock), and K_5 (contact stiffness of bed and ground) have a greater influence on the first eigenfrequency. However, it is difficult to increase K_5 under the condition of limited change of the mass of the holistic machine tool.

Therefore, it is feasible to improve the dynamic performance of the machine tool by increasing K_2 and K_4. Specifically, K_2 can be improved by increasing the contact rate and bolt pre-tightening force of column and bed. As for K_4, the contact area of headstock and column should be increased.

Through the dynamic sensitivity analysis of components and contact parts, the dynamic design optimization strategy of the holistic machine tool is worked out, which is expressed as follows:

(1). Reduce the mass and increase the stiffness of headstock, column, and bed, respectively. The sensitivity magnitudes of headstock are largest, which means optimizing headstock with priority. The following are column and bed.
(2). Increase the contact stiffness of headstock and column, column and bed.

	Mode 1	Mode 2	Mode 3	Mode 4	Mode 5
FEA	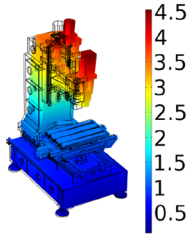	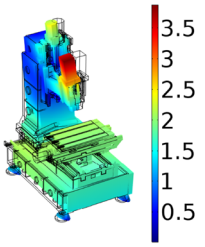	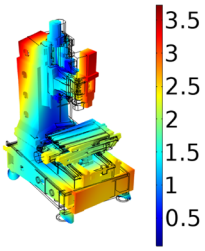	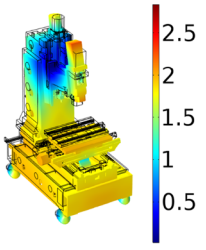	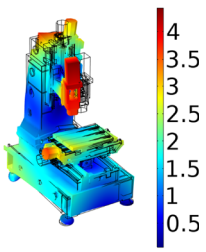
Experiment	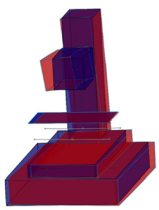	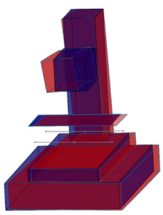	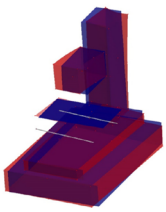	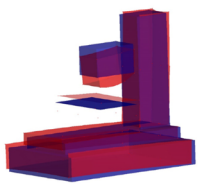	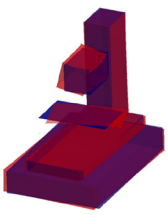
Description	Horizontal movement along X axis, especially the headstock	Horizontal movement along X axis, the same as mode 1	Rotation around Z axis, especially the headstock	Horizontal movement along Z axis, especially the headstock	Rotation around Z axis

Fig. 7 Modal shapes of FEA and experimental models in the lowest 5 modes

Table 2 Eigenfrequency comparison of experimental and FEA models

Mode	Experiment/ Hz	FEA/ Hz	Error/ %
1	37.4	39.3	5.0
2	89.3	89.4	0.1
3	98.3	99.7	1.4
4	134.0	132.0	1.5
5	160.8	147.8	8.1
6	175.5	167.5	4.6

3 Structural topology optimization

3.1 Adaptive Growth Method

Based on the dynamic design optimization strategy, the topology optimization of the components including headstock, column, and bed is conducted by utilizing Adaptive Growth Method, which is a high-efficient effective topology optimization method.

Naturally evolved biological structures exhibit the optimal characteristics of light-weight and high stiffness. Branching systems like plant's root system adapt to their growing environment so that their overall performance in a specific environment is optimized [11]. Based on the growth mechanism of biological branch systems in nature, an optimization method namely Adaptive Growth Method for optimal internal stiffener distribution in three-dimensional box structures is suggested. Under certain boundary conditions, a strain energy field inside a box structure can be compared with the growing environment of a branch network in nature. Adopting the similar principle of growth of a root system, the adaptive growing process of stiffeners in a box structure is depicted in Fig. 9. First, under certain boundary conditions as shown in Fig. 9(a), the seeding lines based on the applied loading and boundary constraints are selected, which is shown in Fig. 9(b). Then, the stiffeners connected with the seeding lines can either grow or degenerate by obeying sensitivity-based iterative rules to achieve an overall strain energy minimum, which are shown in Fig. 9(c), (d). When the stiffeners grow to certain state, they will be "branching," and the adjacent stiffeners can participate in the next growth or branching. Finally, the optimal stiffener layout is obtained as presented in Fig. 9(e). The bottom view of the stiffener layout is shown in Fig. 9(f).

The optimization mathematical model of Adaptive Growth Method is described as

$$\begin{aligned} &\text{find } \mathbf{A} = (A_1, A_2, \cdots A_h \cdots, A_t)^{\mathbf{T}} \\ &\min\ F(\mathbf{A}) = U \\ &\text{s.t. } g(\mathbf{A}) = v - \eta v_0 \le 0 \\ &\quad 0 < A_{\min} \le A_h \le A_{\max} \end{aligned} \tag{12}$$

where A_h is the cross-sectional area of h-th stiffener, which is regarded as the design variable. $A_{\max}$ and $A_{\min}$ are the upper and lower limits of A_h, respectively; t is the total number of stiffeners; objective function U is the overall strain energy; v and v_0 are the actual and initial volume, respectively; η is the volume fraction which should be larger than or equal to 1.

To solve the mathematical optimization model in Eq. 12, the optimality criterion method and KKT conditions are applied [16]. And the update formula of design variables A_h is expressed as

$$A_h^{c+1} = \begin{cases} A_{\min} & \text{if } A_h^c \le A_{\min} \\ \alpha\left(\dfrac{-S_h}{\chi A_h} A_h^c\right) + (1-\alpha) A_h^c & \text{if } A_{\min} < A_h^c < A_{\max} \\ A_{\max} & \text{if } A_h^c \ge A_{\max} \end{cases} \tag{13}$$

where α is the step factor, and χ is the Lagrange multiplier, and S_h is the design sensitivity of the i-th stiffener A_h with respect to the objective function, $S_h = \partial F / \partial A_h$. Equation 13 is

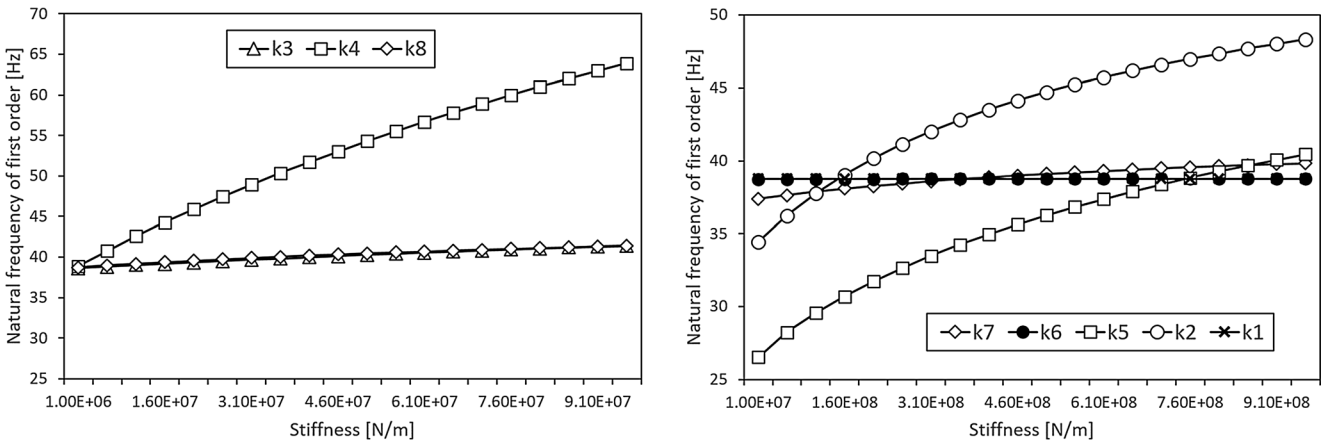

Fig. 8 The sensitivity of the first eigenfrequency with respect to contact stiffness

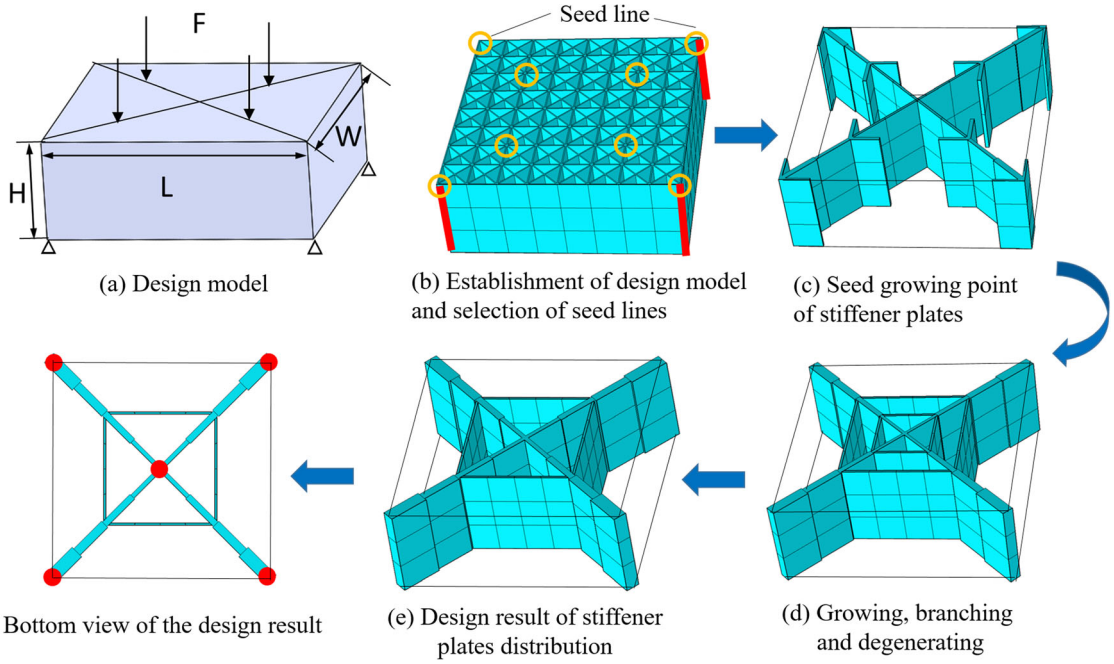

Fig. 9 Design process of Adaptive Growth Method

used as the iterative formula to perform the topology optimization process for the stiffener layout design in a box structure.

3.2 Structural topology optimization of components

The structural topology optimization process of headstock, column, and bed utilizing Adaptive Growth Method is shown in Fig. 10. The objective is the overall strain energy. Boundary conditions and design domains of the three components are shown in Fig. 10(a). As for headstock, four sliding blocks of headstock are constrained, and spindle gravity F_1 is loaded at the front of headstock. The boundary conditions of column are that the bottom of column is constrained, and the gravity of headstock and spindle is loaded at the middle of slide way of column. Considering the working volume of headstock in Z-axis direction, F_2:F_3 = 1:2. As for bed, positions of four sizing blocks are constrained, and the gravities of other components are loaded onto the top surface of bed, and F_4:F_5 = 3:8. The topology iterative process and iterative curves are illustrated in Fig. 10(b), (c), respectively, where N represents the iteration steps. During iteration, structural volumes of headstock, column, and bed increase as the iterative steps increase, and finally converge at N = 65, 134, and 176, respectively. As for column, the topology optimization process of the front and left/right sides is separated; hence, the column structure is symmetric on both sides (left and right sides). It is evident that the stiffener layout of the components is changed.

Employing the topology optimization results, CAD models of the optimal headstock, column, and bed are built, which are shown in Fig. 10(d). Besides, manufacturing constraints are taken into account, such as dimension constraints of stiffeners, draft direction of stiffeners, and guarantee of mounting positions. Compared with the model of original headstock, the biggest difference is that the optimal headstock has an X-type stiffener inside. With regard to column, the stiffener layout of optimal column is changed, and the top half structure is modified, too. The layout of inside stiffeners of optimal bed is changed in the meantime. After optimization, the masses of optimal headstock, column, and bed are decreased by 5.3%, 3.6%, and 0.9%, respectively. In addition, the size of sliding blocks and guides of optimal headstock are increased to improve the contact stiffness of headstock and column.

Then, the structural performance of headstock, column, and bed is evaluated by FEA simulation. The displacement nephogram comparisons of the original and optimal models are shown in Fig. 10(e). The stiffness and eigenfrequency comparisons are listed in Table 3, and the modal shapes are also described. The maximum displacement and first eigenfrequency of optimal headstock are decreased by 33.4% and 29.8%, respectively. Obviously, the static and dynamic performance of headstock is signally improved. The maximum displacement and first eigenfrequency of optimal column are decreased by 14.3% and 12.3%, respectively, which indicates that the performance of column is improved effectively. As for bed, the maximum displacement and first eigenfrequency are decreased by 5.4% and 5.9%, respectively, and the performance of bed is improved slightly.

After the structural topology optimization of headstock, column, and bed, the distributions of mass and stiffness of

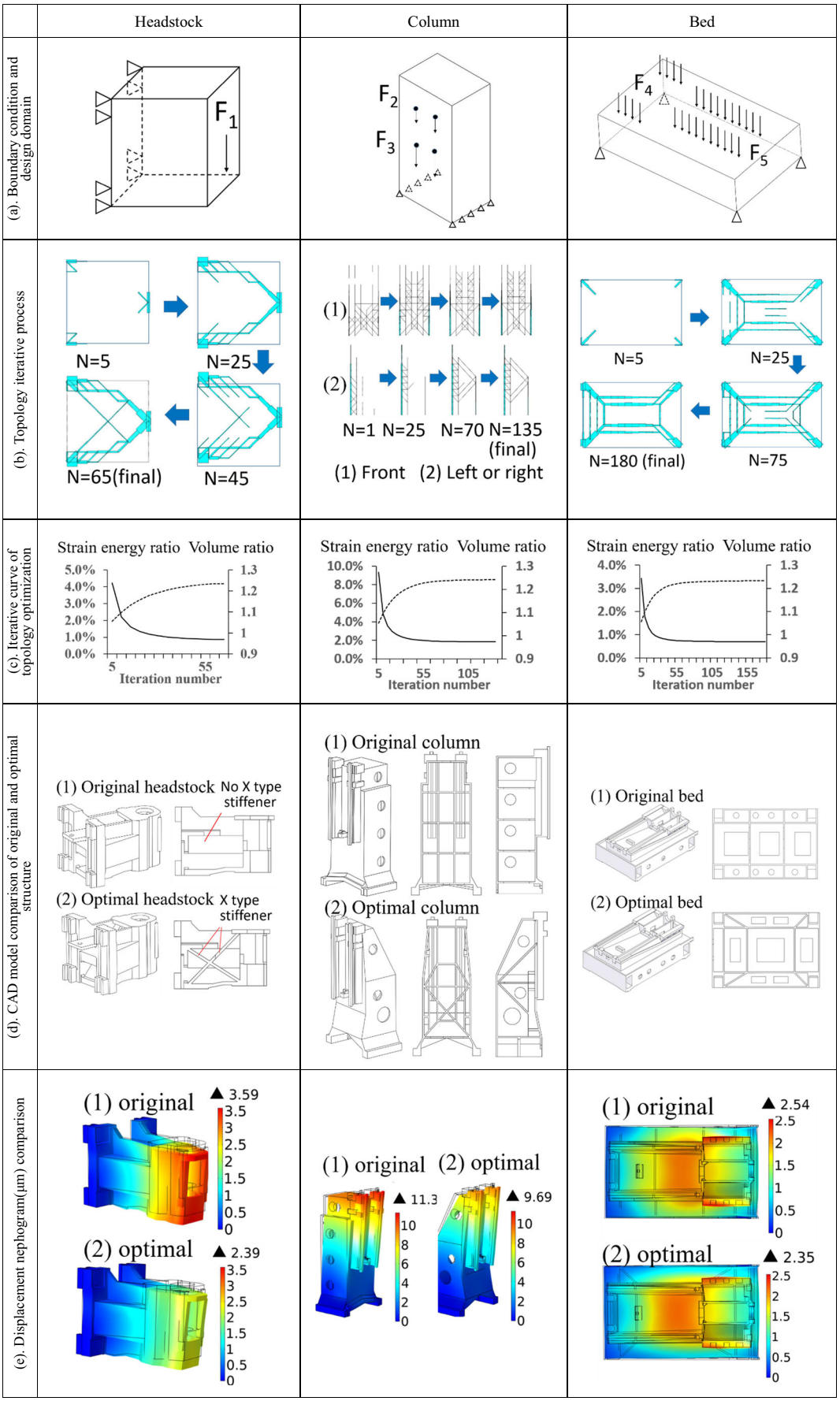

Fig. 10 Topology optimization process of the components utilizing Adaptive Growth Method

Table 3 Performance comparison of the original and optimal components

Component	Performance	Original model	Optimal model	Change (%)
Headstock	Max displacement	3.59 μm	2.39 μm	− 33.4
	Mode 1	506.1 Hz, rotation around *Z*-axis	656.7 Hz, rotation around *X*-axis	+ 29.8
	Mode 2	514.5 Hz, rotation around *X*-axis	667.1 Hz, rotation around *Z*-axis	+ 29.7
	Mode 3	952.3 Hz, torsion	1179.2 Hz, torsion	+ 23.8
Column	Max displacement	4.9 μm	4.2 μm	− 14.3
	Mode 1	118.9 Hz, rotation around *X*-axis	133.8 Hz, rotation around *X*-axis	+ 12.3
	Mode 2	157.8 Hz, rotation around *Y*-axis	178.5 Hz, rotation around *Y*-axis	+ 13.1
	Mode 3	346.5 Hz, torsion	381.6 Hz, torsion	+ 10.1
Bed	Max displacement	2.54 μm	2.35 μm	− 7.5
	Mode 1	339.9 Hz, movement along *Z*-axis	359.8 Hz, movement along *Z*-axis	+ 5.9
	Mode 2	360.8 Hz, movement along *Z*-axis	373.6 Hz, movement along *Z*-axis	+ 3.7
	Mode 3	373.5 Hz, movement along *Y*-axis	408.0 Hz, movement along *Y*-axis	+ 9.4

the components are optimized, and the weak contact stiffness is improved as well.

4 FEA and experimental verifications

4.1 FEA verification

The holistic machine tool structure with optimized components is shown in Fig. 11, and the dynamic performance is first evaluated by FEA simulation. Harmonic force $[10\ 10\ 30]^T$ N is loaded at TCP, and harmonic displacement response of TCP in the frequency range from 0 to 400 Hz is analyzed. Figure 12 shows the TCP harmonic displacement comparison between the original and optimal machine tools, and Table 4 lists the corresponding data. The eigenfrequencies of the optimal machine tool are increased by 6.8%, 3.0%, and 3.8% of the lowest three modes, respectively, and obviously, the TCP harmonic displacement of the optimal machine tool is distinctly decreased. The FEA results indicate that the dynamic performance of the optimal machine tool is improved dramatically.

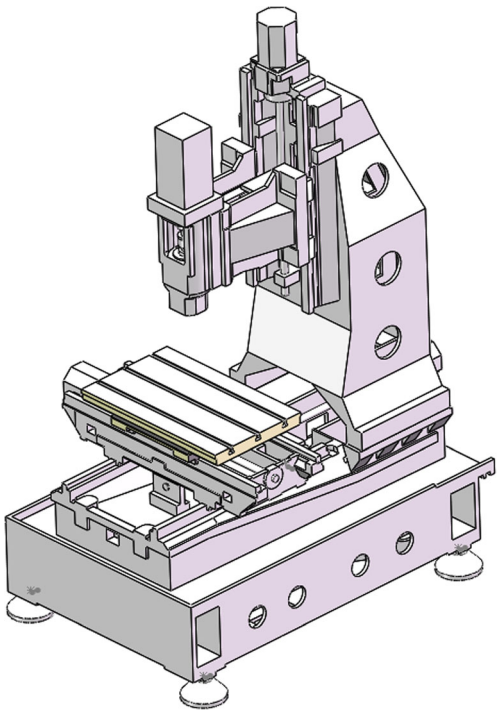

Fig. 11 The optimal machine tool structure

4.2 Experimental verification

For further verification, the optimal machine tool is manufactured. The structural performance of the optimized components is first tested. Due to the fact that the constraint boundary conditions of the components in static and modal tests are difficult to accomplish, the free modal tests are carried out. Onsite free modal tests of the optimal headstock, column, and bed are shown in Fig. 13(a–c). In the tests, the components are hanged by soft ropes and tested by hammering method. The FRFs in *Z*-axis direction are obtained, which are expressed in Fig. 15. Solid and dotted lines represent the original and optimal components, respectively, and the eigenfrequencies of the lowest three modes are marked in the figures. The detailed eigenfrequency comparisons of the three components are listed in Table 5. As seen in the figure and table, the eigenfrequencies of the optimal headstock are increased by 16.8%, 10.8%, and 9.4% in the lowest 3 modes, respectively. Similarity, the eigenfrequencies of the optimal column are increased by 6.7%, 20.7%, and 24.0% respectively in the lowest 3 modes; the eigenfrequencies of the optimal bed are increased by 10.7%, 6.0%, and 23.2% respectively in the

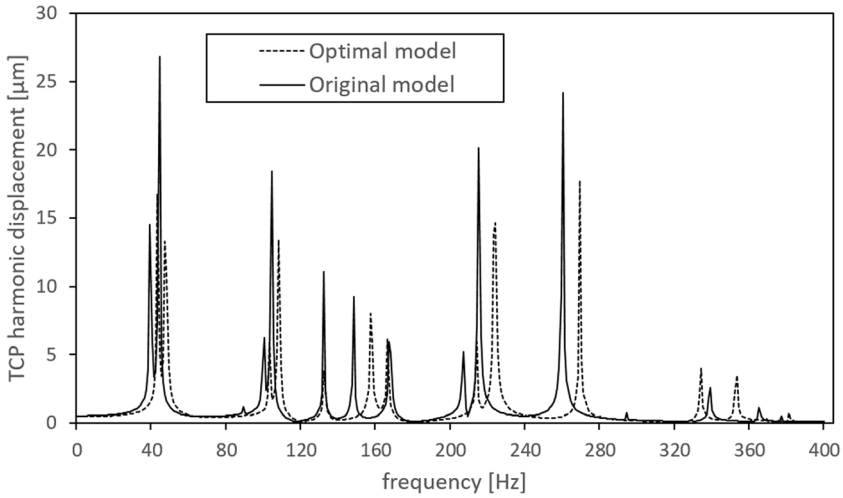

Fig. 12 TCP harmonic response displacement comparison of the original and optimal machine tools

lowest 3 modes. Moreover, the FRF amplitudes of the three components are decreased visibly, especially in the headstock.

It should be noted that the ball screw model of the optimal machine tool structure for headstock and column is changed to increase the contact stiffness as shown in Fig. 14. The ball screw model of the original machine tool is SVR 30R, and the widths of slide block and guide are 60 and 28 mm, respectively; the ball screw model of the optimal machine tool is SVR 35R, and the widths of slide block and guide are 70 and 34 mm, respectively. The change of ball screw model increases the contact area and guarantees the contact stiffness improvement.

Modal test onsite of the optimal holistic machine tool is shown in Fig. 13(d). FRF comparison between the original and optimal machine tools in *Z*-axis direction is shown in Fig. 16, and the eigenfrequency comparison is listed in

Table 4 TCP harmonic response comparison of the original and optimal machine tools

Mode	f_1 (frequency and TCP displacement)	f_2	f_3	f_4	f_5	f_6	f_7	f_8	f_9	f_{10}
Original model	Frequency 39 Hz	44 Hz	100 Hz	104 Hz	132 Hz	148 Hz	167 Hz	207 Hz	215 Hz	260 Hz
	Displacement 14.49 μm	26.8 μm	6.2 μm	18.4 μm	11.1 μm	9.3 μm	5.9 μm	5.2 μm	20.2 μm	24.2 μm
Optimal model	Frequency 43 Hz	47 Hz	103 Hz	108 Hz	132 Hz	157 Hz	166 Hz	214 Hz	224 Hz	269 Hz
	Displacement 16.76 μm	13.3 μm	5.9 μm	13.4 μm	3.8 μm	8.0 μm	6.1 μm	6.0 μm	14.7 μm	17.7 μm
Change	Frequency + 10.3%	+ 6.8%	+ 3.0%	+ 3.8%	+ 0.0%	+ 6.1%	− 0.6%	+ 3.4%	+ 4.2%	+ 3.5%
	Displacement + 15.7%	− 50.5%	− 5.5%	− 27.3%	− 65.7%	− 13.2%	+ 3.8%	+ 14.0%	− 27.4%	− 26.7%

Fig. 13 Modal tests onsite of the optimized machine tool. (a) Bed, (b) column, (c) headstock, and (d) the holistic machine tool

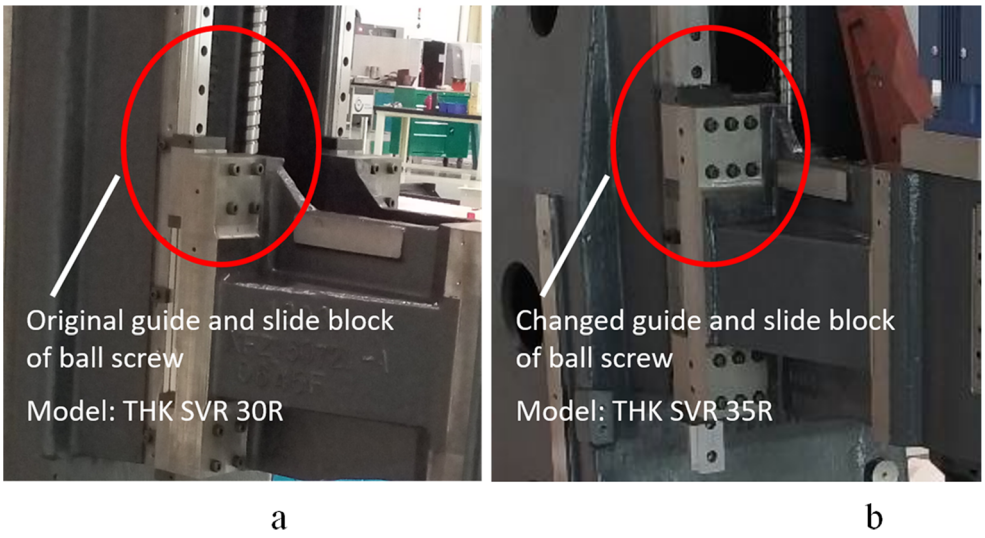

Fig. 14 Ball screw model of the original and optimal machine tool structures for headstock and column. (a) Original machine tool and (b) optimal machine tool

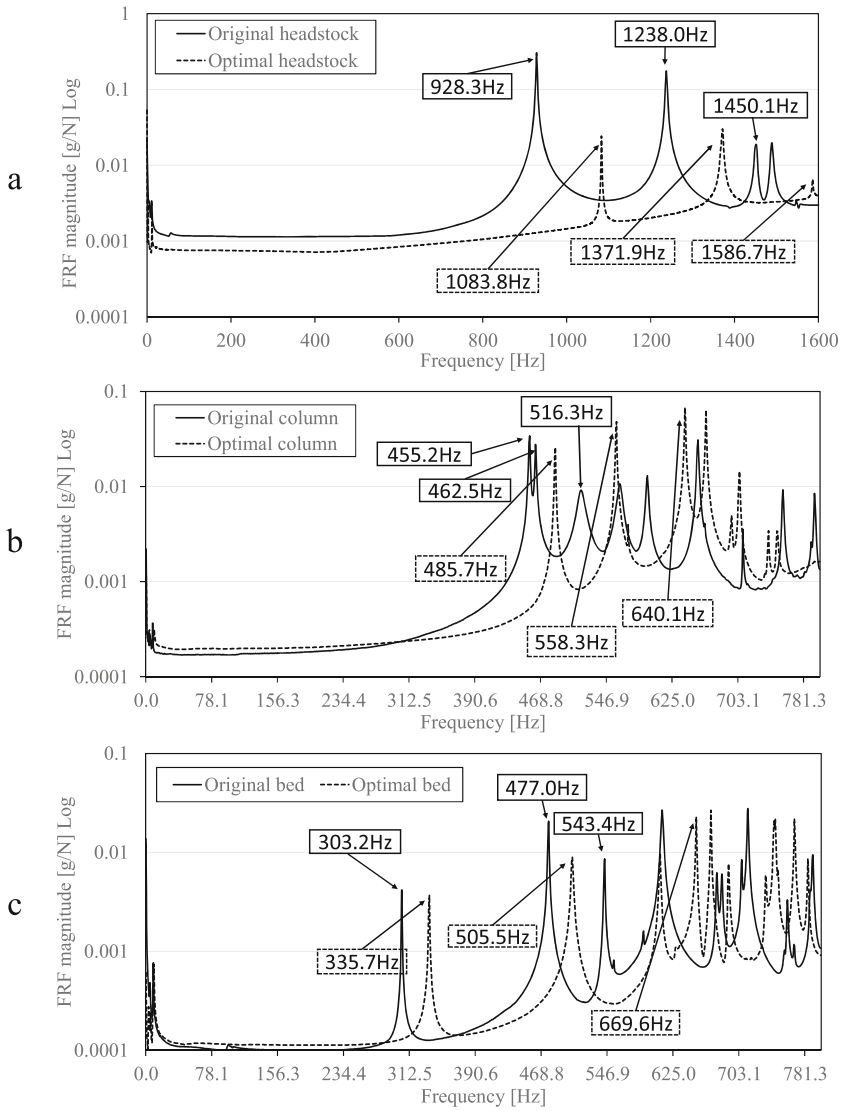

Fig. 15 FRF comparisons of the original and optimal components in *Z*-axis direction. (a) Headstock, (b) column, and (c) bed

Table 5 Eigenfrequency comparisons of the original and optimal machine tools in modal tests (Hz)

Mode	1	2	3	4	5	6
Original headstock	928.3	1238.0	1450.1			
Optimal headstock	1083.8	1371.9	1586.7			
Change	+ 16.8%	+ 10.8%	+ 9.4%			
Original column	455.8	462.5	516.3	563.5	594.9	655.3
Optimal column	482.2	558.3	639.9	664.0	692.5	703.9
Change	+ 5.8%	+ 20.7%	+ 23.9%	+ 17.8%	+ 16.4%	+ 7.4%
Original bed	303.2	477	543.4	612.8	676.7	682.6
Optimal bed	335.7	505.5	609.4	669.6	745.3	768.9
Change	+ 10.7%	+ 6.0%	+ 12.1%	+ 9.3%	+ 10.1%	+ 12.6%
Original machine tool	37.4	89.3	98.3	134.0	160.8	175.5
Optimal machine tool	45.8	102.3	154.5	173.9	181.6	198.6
Change	+ 22.5%	+ 14.6%	+ 57.2%	+ 29.8%	+ 12.9%	+ 13.2%

Table 5. As seen in the table and figure, the eigenfrequencies of the optimal machine tool are increased by 22.5%, 14.6%, and 57.2% in the lowest 3 modes, respectively, and the FRF amplitude is decreased significantly. Although the dynamic performances obtained by FEA results and experiments have a few deviations because of simulation and test errors and different boundary conditions between the simulation and experiment, there is no doubt that the dynamic performance of the optimal machine tool is greatly improved. What needs to be emphasized is that the manufactured optimal machine tool provides strong supportive results.

5 Conclusions

This paper suggests a new dynamic design optimization method by adopting the structural topology design optimization technique and dynamic sensitivity analysis, and both components and contact parts are considered. The dynamic sensitivity analysis of the components based on modal test data helps to determine the weak stiffness and redundant mass; stiffness sensitivity analysis of contact parts with FEA model can identify the weak contact stiffness effectively, and then, the optimization strategy of the holistic machine tool is worked out. For the given vertical machining center, column, headstock, and bed are deemed to the optimization objects. The component rankings for the stiffness improvement and mass reduction are as follows: headstock, column, and bed, and the headstock is optimized with priority. Adaptive Growth Method is then applied to design the layouts of the internal stiffeners of these sensitive components, and the design results are different from the original structures. The stiffness of these components is improved, and the mass is reduced. The weak contact stiffness of headstock and column is increased by changing the ball screw model meanwhile.

After FEM verification, the optimal machine tool is manufactured, and the onsite experiments greatly enhance the effectiveness and feasibility of the suggested design optimization method. The proposed design method can benefit the product-upgrading design of the machine tool and helps to improve the dynamic performance effectively.

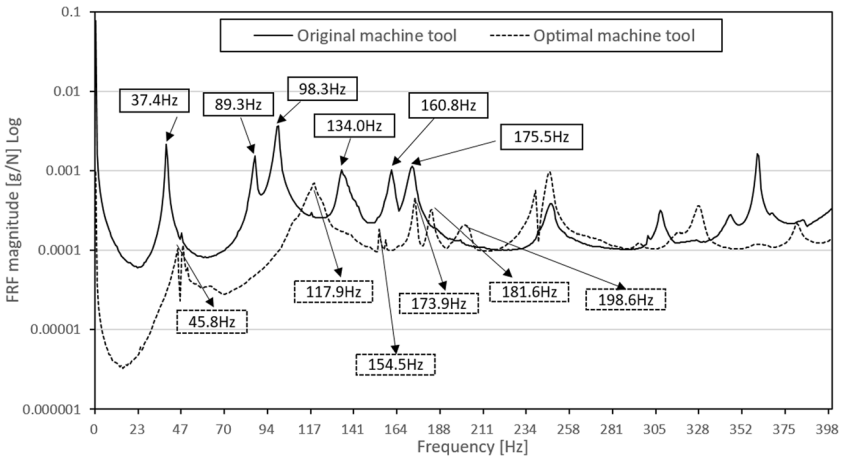

Fig. 16 FRF comparison of the original and optimal machine tools in *Z*-axis direction

Funding information This research is supported by the National Natural Science Foundation of China (Grant No. 51405300) and the Science and Technology Major Special Project of China (Grant No. 2019zx04005-001-010).

References

1. Möhring H-C, Brecher C, Abele E, Fleischer J, Bleicher F (2015) Materials in machine tool structures. CIRP Ann Manuf Technol 64(2):725–748
2. Huo D, Cheng K, Wardle F (2010) A holistic integrated dynamic design and modelling approach applied to the development of ultraprecision micro-milling machines. Int J Mach Tools Manuf 50(4):335–343
3. Liu S (2014) Multi-objective optimization design method for the machine tool's structural parts based on computer-aided engineering. Int J Adv Manuf Technol 78(5–8):1053–1065
4. Shi Y, Zhao X, Zhang H, Nie Y, Zhang D (2015) A new top-down design method for the stiffness of precision machine tools. Int J Adv Manuf Technol 83(9–12):1887–1904
5. Bendsøe MP, Kikuchi N (1988) Generating optimal topologies in structural design using a homogenization method. Comput Methods Appl Mech Eng 71(2):197–224
6. Bendsøe MP, Sigmund O (1999) Material interpolation schemes in topology optimization. Arch Appl Mech 69(9):635–654
7. Drude N, Meier L, Hoffmann H, Scheurle J (2009) Model based strategies for an optimised ribbing design of large forming tools. Prod Eng 3(4):435–440
8. Yun Q, Niu WT, Wang JQ, Zhang L (2013) Structure design of precision horizontal machining center and multi-objective optimization of large structural components. Adv Mater Res 712–715: 1514–1518
9. Chen TY, Wang CB (2008) Topological and sizing optimization of reinforced ribs for a machining centre. Eng Optim 40(1):33–45
10. Law M, Altintas Y, Srikantha Phani A (2013) Rapid evaluation and optimization of machine tools with position-dependent stability. Int J Mach Tools Manuf 68:81–90
11. Dong X, Ding X, Xiong M (2018) Optimal layout of internal stiffeners for three-dimensional box structures based on natural branching phenomena. Eng Optim:1–18.
12. Ding X, Yamazaki K (2004) Stiffener layout design for plate structures by growing and branching tree model (application to vibration-proof design). Struct Multidiscip Optim 26(1):99–110
13. Ding X, Yamazaki K (2005) Adaptive growth technique of stiffener layout pattern for plate and shell structures to achieve minimum compliance. Eng Optim 37(3):259–276
14. Ji J, Ding X, Xiong M (2014) Optimal stiffener layout of plate/shell structures by bionic growth method. Comput Struct 135:88–99
15. Li B, Hong J, Liu Z (2014) Stiffness design of machine tool structures by a biologically inspired topology optimization method. Int J Mach Tools Manuf 84:33–44
16. Zhang H, Ding X, Dong X, Xiong M (2017) Optimal topology design of internal stiffeners for machine pedestal structures using biological branching phenomena. Struct Multidiscip Optim
17. Yan S, Li B, Hong J (2015) Bionic design and verification of high-precision machine tool structures. Int J Adv Manuf Technol 81(1–4):73–85
18. Wu B-C, Young G-S, Huang T-Y (2000) Application of a two-level optimization process to conceptual structural design of a machine tool. Int J Mach Tools Manuf 40(6):783–794
19. Wang J, Niu W, Ma Y, Xue L, Cun H, Nie Y, Zhang D (2016) A CAD/CAE-integrated structural design framework for machine tools. Int J Adv Manuf Technol 91(1–4):545–568
20. Li W, Li B, Yang J (2017) Design and dynamic optimization of an ultra-precision micro grinding machine tool for flexible joint blade machining. Int J Adv Manuf Technol 93(9–12):3135–3147
21. He S, Mao X, Liu X, Luo B, Li B, Peng F (2015) A new approach based on modal mass distribution matrix to identify weak components of machine tool structure. Int J Adv Manuf Technol 83(1–4): 193–203
22. Liang Y, Chen W, Sun Y, Luo X, Lu L, Liu H (2013) A mechanical structure-based design method and its implementation on a fly-cutting machine tool design. Int J Adv Manuf Technol 70(9–12): 1915–1921
23. Chen W, Liang Y, Sun Y, Huo D, Lu L, Liu H (2013) Design philosophy of an ultra-precision fly cutting machine tool for KDP crystal machining and its implementation on the structure design. Int J Adv Manuf Technol 70(1–4):429–438
24. Li TJ, Ding XH, Cheng K, Wu T (2017) Dynamic optimization method with applications for machine tools based on approximation model. P I Mech Eng C-J Mec 232(11):2009–2022
25. Zhao L, Chen H, Yao Y, Diao G (2016) A new approach to improving the machining precision based on dynamic sensitivity analysis. Int J Mach Tools Manuf 102:9–21
26. Zhang GP, Huang YM, Shi WH, Fu WP (2003) Predicting dynamic behaviours of a whole machine tool structure based on computer-aided engineering. Int J Mach Tools Manuf 43(7):699–706
27. Deng C, Yin G, Fang H, Meng Z (2015) Dynamic characteristics optimization for a whole vertical machining center based on the configuration of joint stiffness. Int J Adv Manuf Technol 76(5): 1225–1242
28. Hung J-P, Lai Y-L, Lin C-Y, Lo T-L (2011) Modeling the machining stability of a vertical milling machine under the influence of the preloaded linear guide. Int J Mach Tools Manuf 51(9):731–739
29. Hung JP, Lai YL, Luo TL, Su HC (2013) Analysis of the machining stability of a milling machine considering the effect of machine frame structure and spindle bearings: experimental and finite element approaches. Int J Adv Manuf Technol 68(9–12):2393–2405